

Noncoherent ISAC over Block-Fading Channels: Asymptotic Performance Analysis

Hao Yang*, Kai Wan*, Giuseppe Caire[†]

*Huazhong University of Science and Technology, 430074 Wuhan, China, {hao_yang,kai_wan}@hust.edu.cn

[†]Technische Universität Berlin, 10587 Berlin, Germany, caire@tu-berlin.de

Abstract—This paper investigates the fundamental limits and optimal signal distribution design for Integrated Sensing and Communication (ISAC) systems operating under strictly noncoherent conditions. Unlike conventional coherent frameworks that rely on perfect channel state information, we consider a block-fading MIMO channel where the channel realizations are unknown to both the transmitter and the receiver. We adopt a realization-wise perspective to characterize the noncoherent performance tradeoff across different signal-to-noise ratio (SNR) regimes. In the high-SNR regime, we derive a lower bound for the noncoherent mutual information and define a metric, termed sensing-induced rate loss, to quantify the communication penalty incurred by sensing-oriented beamforming. We then employ a projected gradient algorithm to optimize the spatial power allocation, balancing the conflict between the unitary space-time modulation-based structure for communication and the task-oriented spatial power allocation for sensing. Conversely, in the low-SNR regime, we perform a first-order asymptotic analysis of the ergodic minimum mean squared error (EMMSE). Our theoretical derivation reveals a fundamental synergy: the sensing-optimal strategy collapses to a rank-one transmission along the dominant eigenvector of the target response, which incurs no first-order communication loss in the low-SNR regime. This result demonstrates that the conflicting tradeoff observed at high SNR vanishes asymptotically at low SNR, enabling perfect alignment between sensing and communication objectives.

Index Terms—Integrated sensing and communication, noncoherent communication, block-fading, EMMSE.

I. INTRODUCTION

The paradigm of Integrated Sensing and Communication (ISAC) has emerged as a transformative architecture for future wireless networks, predicated on the synergistic integration of hardware and spectral resources. To date, the majority of information-theoretic milestones in ISAC have been established under the assumption of a coherent regime, where perfect channel state information (CSI) is presumed to be available at both the transmitter and receiver [1]–[3]. Within this coherent framework, extensive research has been devoted to characterizing the Pareto boundary between communication mutual information and sensing performance, quantified via Bayesian Cramér-Rao bound (BCRB)-based metrics (e.g., [1], [4]) or minimum mean squared error (MMSE)-type metrics [5], [6], while alternative formulations based on sensing mutual information have also been proposed [7]. However, these idealized gains often hinge on the implicit assumption that the resources dedicated to channel training and feedback are negligible—a premise that inevitably collapses in highly dynamic or power-constrained environments. Consequently, investigating

ISAC systems under strictly noncoherent conditions—where instantaneous channel realizations remain unknown to all nodes—is of paramount importance for characterizing the fundamental limits of practical deployments.

Building upon these coherent results, recent literature has shifted toward optimizing ISAC systems under more realistic CSI configurations and signaling constraints. For instance, the authors in [8] showed that in a state-dependent multi-access channel (MAC) with generalized feedback, the lack of instantaneous CSI at the transmitters requires carefully designed signaling strategies, even when the receiver observes the channel outputs perfectly. Furthermore, investigations into signal shaping [9], [10] have exposed a critical divergence between deterministic and random signaling: while Gaussian stochasticity is conventionally optimal for communication capacity, its inherent uncertainty may compromise sensing resolution. This tension necessitates a judicious balance in the design of the underlying signal structure.

At a more fundamental level, the information-theoretic framework for noncoherent joint transmission and state sensing was pioneered by Zhang *et al.* [11], who conceptualized the sensing task through the lens of a state-dependent memoryless channel. By assuming the state is unknown to both terminal nodes, they characterized the tradeoff between the achievable communication rate and state estimation distortion. This framework was subsequently refined by Choudhuri *et al.* [12], who incorporated causal and strictly causal state information at the transmitter, thereby establishing the analytical basis for evaluating how asymmetric environmental knowledge dictates system performance bounds. Related formulations consider fixed but unknown channel states and use a detection-error exponent as the sensing metric; see, e.g., Chang *et al.* [13], who characterized the rate–detection-exponent tradeoff for joint communication and sensing of discrete channel states.

Despite these advances, the optimal design for strictly noncoherent ISAC remains under-explored, particularly regarding the influence of the signal-to-noise ratio (SNR) regime. In the high-SNR regime, the noncoherent channel is primarily degree of freedom limited; here, enforcing a sensing-optimal covariance structure creates a structural mismatch with the capacity-achieving unitary space-time modulation (USTM) profile characterized by [14], [15], leading to a quantifiable capacity penalty. In stark contrast, the low-SNR regime is power-limited [16], where the stringent requirements for spatially uniform signaling relax as the capacity scales linearly with

the total received power. This observation raises the question of whether the sensing and communications (S&C) tradeoff persists across all power regimes. Specifically, it remains to be determined whether the structural conflict observed at high SNR is fundamental, or if the two objectives asymptotically align in the low-SNR regime, enabling synergistic operation.

Motivated by these considerations, this paper investigates the optimization of ISAC systems operating under strictly noncoherent conditions. We consider a block-fading MIMO Gaussian channel, where the channel matrix remains constant over a coherence interval of T symbols but its realization is unknown to all nodes. Our contributions are three-fold:

- *Optimal signaling structure:* We derive the fundamental signal structure for noncoherent ISAC systems. We prove that the optimal sensing strategy—a deterministic sample covariance aligned with the target’s eigen-structure—admits an *effective communication input* representation. By exploiting the unitary invariance of isotropic block-fading channels, we demonstrate that the spatial rotation required for sensing is transparent to the communication receiver. This structural insight rigorously reduces the joint design from complex matrix optimization to tractable power allocation over spatial eigenmodes.

- *High-SNR tradeoff and rate loss quantification:* We derive a high-SNR lower bound on the noncoherent mutual information for block-fading MIMO channels. Based on this bound, we introduce the *sensing-induced rate loss* to quantify the penalty incurred by deviating from equal-power signaling (i.e., USTM) to satisfy sensing-specific requirements. Consequently, we formulate a convex optimization problem for spatial power allocation to trace the system’s Pareto frontier.

- *Low-SNR asymptotic alignment:* We prove analytically that the sensing-optimal strategy collapses to a rank-one beamforming along the dominant eigenmode of the target. Crucially, our analysis reveals that this highly structured transmission incurs no penalty in the first-order communication rate, as the noncoherent capacity becomes insensitive to the spatial covariance structure in this regime. This highlights an interesting phenomenon: the conflicting tradeoff observed at high SNR vanishes asymptotically at low SNR, allowing for perfect alignment of S&C objectives.

Notations: x , \mathbf{x} , and \mathbf{X} represent random variables, random vectors, and random matrices, respectively, with their deterministic counterparts denoted by x , \mathbf{x} , and \mathbf{X} . The $M \times M$ identity matrix is denoted by \mathbf{I}_M . $\mathbb{E}[\cdot]$ and $\mathbb{P}[\cdot]$ denote the expectation and probability operators, respectively. The transpose and Hermitian transpose are denoted by $[\cdot]^T$ and $[\cdot]^H$, respectively. $[\mathbf{X}]_{ij}$ denotes the (i, j) -th entry of matrix \mathbf{X} . $\text{diag}(\mathbf{x})$ denotes a diagonal matrix with the elements of \mathbf{x} on its main diagonal, and $\text{tr}(\cdot)$ denotes the trace of a matrix. $\mathbf{A} \succeq \mathbf{B}$ indicates that $\mathbf{A} - \mathbf{B}$ is positive semidefinite.

II. SYSTEM MODEL AND PRELIMINARIES

A. System Model

Let us consider the general ISAC system model given by

$$\mathbf{Y}_i = \mathbf{H}_i \mathbf{X} + \mathbf{Z}_i, \quad i \in \{c, s\}, \quad (1)$$

where $\mathbf{H}_c \in \mathbb{C}^{N_c \times M}$ and $\mathbf{H}_s \in \mathbb{C}^{N_s \times M}$ denote the communication channel and the target response matrix, respectively, with M , N_c , and N_s being the number of antennas at the ISAC transmitter (Tx), the communication receiver (Rx1), and the sensing receiver (Rx2), respectively. $\mathbf{Y}_c \in \mathbb{C}^{N_c \times T}$ and $\mathbf{Y}_s \in \mathbb{C}^{N_s \times T}$ denote the received communication and sensing signals over a coherence block of length T , respectively. $\mathbf{X} \in \mathbb{C}^{M \times T}$ denotes the transmitted dual-functional waveform for performing both S&C tasks. In this paper, we assume that \mathbf{X} is known to both the Tx and Rx2 (e.g., as is typical in monostatic sensing setups or bistatic systems with perfect backhaul), but is unknown to Rx1. Neither the Tx nor Rx1 has access to realizations of \mathbf{H}_c , and each element of \mathbf{H}_c , h_{ij} for $i = 1, \dots, N_c$ and $j = 1, \dots, M$, is assumed to be independently and identically distributed (i.i.d.) zero-mean circularly symmetric complex Gaussian with unit variance, i.e., $h_{ij} \sim \mathcal{CN}(0, 1)$. The noise matrices \mathbf{Z}_c and \mathbf{Z}_s have i.i.d. $\mathcal{CN}(0, \sigma_c^2)$ and $\mathcal{CN}(0, \sigma_s^2)$ entries, respectively. The communication subsystem aims at transmitting as much information as possible (reliably) to Rx1, while the sensing subsystem aims at estimating \mathbf{H}_s at Rx2.

We consider a block-fading model for both the sensing channel and the communication channel. Specifically, we assume that \mathbf{H}_s varies every T symbols in an i.i.d. manner, following a statistical correlation matrix $\mathbf{R}_{\mathbf{H}_s} = \mathbb{E}[\mathbf{H}_s^H \mathbf{H}_s]$, and that the communication channel \mathbf{H}_c also varies every T symbols in an i.i.d. manner. We will refer to T as the *coherence time*¹ in the rest of the paper. In this strictly noncoherent setting, no terminal has access to the instantaneous realizations of \mathbf{H}_c or \mathbf{H}_s ; only their distributions and, for sensing, the second-order statistics $\mathbf{R}_{\mathbf{H}_s}$ are assumed known.

The average transmit power at each transmit antenna in one symbol period is normalized to 1, and thus the power constraint can be written as

$$\mathbb{E}[\text{tr}(\mathbf{X}\mathbf{X}^H)] = MT. \quad (2)$$

We refer to the SNR as the average SNR at each receive antenna. Under the aforementioned normalization, the communication SNR and sensing SNR are respectively defined as

$$\text{SNR}_c \triangleq \frac{M}{\sigma_c^2} \quad \text{and} \quad \text{SNR}_s \triangleq \frac{M}{\sigma_s^2}. \quad (3)$$

The performance of the communication subsystem is conventionally characterized by

$$C = \sup_{p_{\mathbf{X}}(\mathbf{X})} T^{-1} I(\mathbf{Y}_c; \mathbf{X}), \quad \text{s.t. } p_{\mathbf{X}}(\mathbf{X}) \in \mathcal{F}, \quad (4)$$

where $I(\mathbf{Y}_c; \mathbf{X})$ denotes the mutual information between \mathbf{Y}_c and \mathbf{X} , and \mathcal{F} denotes the feasibility region of $p_{\mathbf{X}}(\mathbf{X})$ determined by the power constraint (2).

We utilize the ergodic MMSE (EMMSE)² to quantify sensing performance [17]. This metric is formulated based on the linear

¹This identical coherence time assumption is standard in information-theoretic ISAC studies (cf. [1]–[3]) to model scenarios where targets and users share similar mobilities. Extending to dual-timescale models ($T_c \neq T_s$) breaks the required unitary invariance and is left for future work.

²We adopt EMMSE because it leads to a more tractable optimization framework and remains a tighter performance indicator in the low-SNR noncoherent regime, where derivative-based bounds like the BCRB often become overly optimistic or difficult to compute.

MMSE estimator, under the assumption that channel statistics are known. The ergodic estimation error can be computed as

$$J_{\text{EMMSE}} \triangleq \mathbb{E}_{\mathbf{X}} \left[\text{tr} \left((\mathbf{R}_{\mathbf{H}_s}^{-1} + \kappa \mathbf{X} \mathbf{X}^H)^{-1} \right) \right] \quad (5a)$$

$$= \mathbb{E}_{\mathbf{R}_{\mathbf{X}}} \left[\text{tr} \left((\mathbf{R}_{\mathbf{H}_s}^{-1} + \kappa T \mathbf{R}_{\mathbf{X}})^{-1} \right) \right], \quad (5b)$$

where $\kappa = 1/\sigma_s^2 N_s = \text{SNR}_s / M N_s$ and $\mathbf{R}_{\mathbf{X}} = T^{-1} \mathbf{X} \mathbf{X}^H$ is the sample covariance matrix, and $\mathbf{R}_{\mathbf{H}_s}$ is assumed to be full-rank, so that $\mathbf{R}_{\mathbf{H}_s}^{-1}$ exists.

B. Preliminary Results on Noncoherent Communication

For noncoherent communication models where the fading coefficients are unavailable at both the receiver and the transmitter (i.e., by removing the sensing task from our considered problem), the channel capacity has been characterized in [15], [18]. We recall the main structural results as follows.

Definition 1 ([15]). *A random matrix $\mathbf{R} \in \mathbb{C}^{M \times T}$, for $T \geq M$, is called isotropically distributed (i.d.) if $p(\mathbf{R}) = p(\mathbf{R}\mathbf{U})$ for any deterministic $T \times T$ unitary matrix \mathbf{U} .*

Lemma 1 ([15]). *Let \mathbf{H} be i.d., and let \mathbf{U} be a random unitary matrix independent of \mathbf{H} . Then, for any realization $\mathbf{U} = \mathbf{U}$, the distribution of $\mathbf{H}\mathbf{U}$ is identical to that of \mathbf{H} . Accordingly, $\mathbf{H}\mathbf{U}$ and \mathbf{U} are statistically independent.*

Lemma 2 ([18]). *The input distribution that achieves capacity can be written as $\mathbf{X} = \mathbf{A}\mathbf{Q}$, where \mathbf{Q} is an $M \times T$ i.d. semi-unitary matrix, i.e., $\mathbf{Q}\mathbf{Q}^H = \mathbf{I}_M$, and \mathbf{A} is an $M \times M$ real diagonal random matrix. Moreover, \mathbf{A} and \mathbf{Q} are independent.*

This characterization reduces the optimization dimensionality from MT to M . At high SNR, the equal-power input $\mathbb{P}[\mathbf{A} = \sqrt{T} \mathbf{I}_M] = 1$ is asymptotically optimal, yielding explicit expressions for the high-SNR capacity derived in [15].

Lemma 3 ([15]). *For the noncoherent MIMO channel with $M \leq N_c$ and $T \geq N_c + M$, the high-SNR capacity is*

$$C_{\text{pure}} = M \left(1 - \frac{M}{T} \right) \log_2 \text{SNR}_c + c + o(1), \quad (6)$$

where

$$c = \frac{1}{T} \log_2 |G(T, M)| + M \left(1 - \frac{M}{T} \right) \log_2 \frac{T}{M\pi e} + \left(1 - \frac{M}{T} \right) \mathbb{E}[\log_2 \det \mathbf{H}_c^H \mathbf{H}_c],$$

with $|G(T, M)|$ denoting the volume of the complex Grassmann manifold $G(T, M)$.

III. SENSING-OPTIMAL DESIGN AND EFFECTIVE COMMUNICATION INPUT

In this section, we establish the fundamental signaling structure for the noncoherent ISAC system. We first derive the sensing-optimal transmit strategy and then connect it to the noncoherent communication framework. Exploiting the unitary invariance of the isotropic communication channel, we show that the spatial rotation required for sensing is transparent to communication, so that the joint design reduces to a tractable optimization over spatial power allocation.

A. Sensing-Optimal Design

Proposition 1. *To minimize the J_{EMMSE} under the power constraint (2), the optimal transmit signal \mathbf{X}^* must satisfy:*

- 1) *The sample covariance matrix $\mathbf{R}_{\mathbf{X}}$ is deterministic.*
- 2) *The optimal sample covariance follows the structure*

$$\mathbf{R}_{\mathbf{X}}^* = \mathbf{U}_s (\mathbf{D}_s^*)^2 \mathbf{U}_s^H, \quad (7)$$

where \mathbf{U}_s is the unitary eigenvector matrix of $\mathbf{R}_{\mathbf{H}_s} = \mathbf{U}_s \mathbf{\Lambda}_s \mathbf{U}_s^H$.

- 3) *Water-filling Power Allocation: The i -th diagonal element of $(\mathbf{D}_s^*)^2$, denoted by $(d_i^*)^2$, $d_i \geq 0$, is given by*

$$(d_i^*)^2 = \frac{1}{\kappa T} \left(\nu - \frac{1}{\lambda_i} \right)^+, \quad \forall i \in \{1, \dots, M\}, \quad (8)$$

where λ_i is the i -th eigenvalue of $\mathbf{R}_{\mathbf{H}_s}$, and $\nu \geq 0$ is the Lagrange multiplier ensuring $\sum_{i=1}^M (d_i^*)^2 = M$.

- 4) *If \mathbf{H}_s is i.d., then $\mathbf{R}_{\mathbf{H}_s} \propto \mathbf{I}_M$ and $d_i^* = 1, \forall i$.*

Proof. (sketch) Convexity of J_{EMMSE} with respect to $\mathbf{R}_{\mathbf{X}}$ and Jensen's inequality imply that the optimal $\mathbf{R}_{\mathbf{X}}$ is deterministic. Eigenvector alignment and the water-filling structure follow from standard trace inequalities and KKT conditions. For a detailed proof, please refer to Appendix A. \square

B. Effective Communication Input

Note that Proposition 1 only imposes a constraint on the sample covariance matrix, implying that the sensing-optimal transmit signal is not unique. To simultaneously fulfill this sensing requirement and the noncoherent capacity-achieving structure in Lemma 2, a structurally compatible transmit signal is constructed as $\mathbf{X}^* = \sqrt{T} \mathbf{U}_s \mathbf{D}_s^* \mathbf{Q}$, where \mathbf{D}_s^* is defined in Proposition 1 and \mathbf{Q} is Haar-distributed semi-unitary. In isotropic scattering environments, the communication channel \mathbf{H}_c is i.d.. By Lemma 1, we have

$$\mathbf{H}_c \mathbf{X}^* = \sqrt{T} (\mathbf{H}_c \mathbf{U}_s) \mathbf{D}_s^* \mathbf{Q} \stackrel{\text{d}}{=} \sqrt{T} \mathbf{H}_c \mathbf{D}_s^* \mathbf{Q},$$

where $\stackrel{\text{d}}{=}$ denotes equality in distribution. This equivalence indicates that the unitary precoder \mathbf{U}_s designed for sensing eigenspace alignment is completely absorbed into the channel distribution and thus does not affect the ergodic communication rate. Consequently, from the communication perspective, the effective input under the sensing-optimal design is given by

$$\mathbf{X}_{\text{eff}}^* = \sqrt{T} \mathbf{D}_s^* \mathbf{Q}. \quad (9)$$

Comparing this with the general representation $\mathbf{X} = \mathbf{A}\mathbf{Q}$ in Lemma 2, we see that a sensing-optimal choice within this class is to take a deterministic diagonal matrix

$$\mathbf{A}_s^* \triangleq \sqrt{T} \mathbf{D}_s^*. \quad (10)$$

In the subsequent joint design, we restrict attention to transmit signals of the form $\mathbf{X} = \mathbf{A}\mathbf{Q}$ in Lemma 2, and model the diagonal matrix as a *deterministic* design variable within each coherence block. That is, we set $\mathbf{A} = \mathbf{A}$ a.s. for a generic diagonal matrix $\mathbf{A} \succeq \mathbf{0}$ (possibly different from \mathbf{A}_s^*), while the randomness of the input is entirely carried by \mathbf{Q} . Furthermore, based on the unitary invariance of both the sensing metric and the i.d. communication channel, it is without loss of generality to work in the *eigen-basis* of $\mathbf{R}_{\mathbf{H}_s}$. That is, we can rotate the coordinate system by \mathbf{U}_s so that $\mathbf{R}_{\mathbf{H}_s}$ becomes diagonal, and

the design reduces to optimizing the diagonal entries of \mathbf{A} over M parallel spatial streams.

IV. OPTIMAL DESIGN AND PERFORMANCE ANALYSIS IN HIGH AND LOW SNR REGIMES

We now investigate the optimal signaling strategy for the considered noncoherent ISAC system. Our goal is to characterize the structure of the transmit signal \mathbf{X} that balances the conflicting requirements of sensing and communication.

A. Asymptotic Analysis in the High-SNR Regime

In this subsection, we consider the high-SNR regime.

Proposition 2. *In the high-SNR regime, the noncoherent mutual information $I(\mathbf{X}; \mathbf{Y}_c)$ is lower-bounded as*

$$I(\mathbf{X}; \mathbf{Y}_c) \geq (T - M)\mathbb{E} [\log \det(\mathbf{A}^2)] + \hat{c} + o(1). \quad (11)$$

Proof.

$$\begin{aligned} I(\mathbf{X}; \mathbf{Y}_c) &= h(\mathbf{Y}_c) - h(\mathbf{Y}_c | \mathbf{X}) \\ &\stackrel{(a)}{=} h(\mathbf{H}_c \mathbf{A} \Psi) + (T - M - N_c)\mathbb{E} [\log \det(\mathbf{A}^2)] + c_0 + o(1) \\ &\stackrel{(b)}{=} h(\mathbf{H}_c \mathbf{A} \Psi | \mathbf{A}, \Psi) + I(\mathbf{H}_c \mathbf{A} \Psi; \mathbf{A}, \Psi) \\ &\quad + (T - M - N_c)\mathbb{E} [\log \det(\mathbf{A}^2)] + c_0 + o(1) \\ &\stackrel{(c)}{=} \mathbb{E} [N_c \log \det(\pi e \mathbf{A}^2)] + I(\mathbf{H}_c \mathbf{A} \Psi; \mathbf{A}) + I(\mathbf{H}_c \mathbf{A} \Psi; \Psi | \mathbf{A}) \\ &\quad + (T - M - N_c)\mathbb{E} [\log \det(\mathbf{A}^2)] + c_0 + o(1) \\ &\stackrel{(d)}{=} (T - M)\mathbb{E} [\log \det(\mathbf{A}^2)] + I(\mathbf{H}_c \mathbf{A} \Psi; \mathbf{A}) \\ &\quad + I(\mathbf{H}_c \mathbf{A} \Psi; \Psi | \mathbf{A}) + \hat{c} + o(1) \\ &\stackrel{(e)}{\geq} (T - M)\mathbb{E} [\log \det(\mathbf{A}^2)] + \hat{c} + o(1) \triangleq I_{\text{lb}}(\mathbf{A}), \end{aligned} \quad (12)$$

where (a) follows from the high-SNR asymptotic expansion in [15, Eq. (25) and subsequent equations] with c_0 denoting all terms independent of \mathbf{A} , and $\Psi \in \mathbb{C}^{M \times M}$ is an auxiliary i.i.d. unitary matrix independent of \mathbf{H}_c and \mathbf{A} ; (b) applies the entropy decomposition; (c) conditions on (\mathbf{A}, Ψ) and evaluates the resulting Gaussian entropy, yielding $h(\mathbf{H}_c \mathbf{A} \Psi | \mathbf{A}, \Psi) = \mathbb{E}[N_c \log \det(\pi e \mathbf{A}^2)]$; (d) collects all \mathbf{A} -dependent terms and absorbs constants into \hat{c} ; and (e) follows from the non-negativity of mutual information. \square

In particular, if \mathbf{A} is deterministic, then $I(\mathbf{H}_c \mathbf{A} \Psi; \mathbf{A}) = 0$. Moreover, in the communication-optimal case where $\mathbf{A} = \sqrt{T} \mathbf{I}_M$ a.s., we have $I(\mathbf{H}_c \mathbf{A} \Psi; \Psi | \mathbf{A}) = 0$, since $\sqrt{T} \mathbf{H}_c \Psi$ is independent of Ψ under i.i.d. \mathbf{H}_c (cf. Lemma 1). Hence, the lower bound in (11) is tight in this case.

To characterize the impact of sensing-driven deviations from uniform power allocation in noncoherent ISAC systems, we transition from the statistical bound in Proposition 2 to a structure-aware metric.

Definition 2. *For any given $\mathbf{A} \succeq \mathbf{0}$ satisfying $\text{tr}(\mathbf{A}^2) = MT$, the sensing-induced rate loss is*

$$\begin{aligned} \Delta(\mathbf{A}) &\triangleq C_{\text{pure}} - T^{-1} I_{\text{lb}}(\mathbf{A}) \\ &= \left(1 - \frac{M}{T}\right) (M \log T - \log \det(\mathbf{A}^2)), \end{aligned} \quad (13)$$

where C_{pure} denotes the achievable high-SNR rate attained by $\mathbf{A}^* = \sqrt{T} \mathbf{I}_M$ (cf. Lemma 3), and $I_{\text{lb}}(\mathbf{A})$ is the lower bound obtained by evaluating (12) at the realization $\mathbf{A} = \mathbf{A}$.

Theorem 1. *The sensing-induced rate loss $\Delta(\mathbf{A}) \geq 0$ for all feasible \mathbf{A} , with equality if and only if $\mathbf{A}^2 = T \mathbf{I}_M$.*

Proof. By applying the Arithmetic-Geometric Mean inequality, $\frac{1}{M} \log \det(\mathbf{A}^2) = \frac{1}{M} \sum_{i=1}^M \log[\mathbf{A}]_{ii}^2 \leq \log\left(\frac{1}{M} \sum_{i=1}^M [\mathbf{A}]_{ii}^2\right) = \log T$. Thus, $\Delta \geq 0$, with equality holding if and only if all $[\mathbf{A}]_{ii}$ are equal, i.e., $\mathbf{A}^2 = T \mathbf{I}_M$. \square

Remark 1. *Within the considered noncoherent ISAC framework, a favorable structural compatibility emerges:*

- **Structural Compatibility:** *When \mathbf{A} is deterministic, the semi-unitary constraint $\mathbf{Q}\mathbf{Q}^H = \mathbf{I}_M$ ensures that the covariance $\mathbf{R}_{\mathbf{X}} = T^{-1} \mathbf{A}^2$ is independent of \mathbf{Q} . As a result, the sensing performance depends only on the second-order statistics of the transmit signal and is decoupled from the specific realizations of the random communication symbols.*

- **Tradeoff Vanishing:** *While noncoherent communication favors equal-power signaling ($\mathbf{X} = \sqrt{T} \mathbf{Q}$) in the high-SNR regime, the sensing-optimal design reduces to the same structure when the sensing channel is isotropic ($\mathbf{R}_{\mathbf{H}_s} \propto \mathbf{I}_M$) (cf. Proposition 1). Consequently, under isotropic sensing environments and high-SNR asymptotics, the design objectives for S&C become structurally compatible, implying that the tradeoff vanishes under the adopted performance metrics.*

Building on the sensing-induced rate loss metric defined above and the effective communication input representation developed in Subsection III-B, the joint S&C design can be formulated as a tradeoff between the rate penalty and the sensing error. Since the problem is fully parameterized by the diagonal power allocation matrix $\hat{\mathbf{A}} = \mathbf{A}^2 = \text{diag}(\hat{a}_1, \dots, \hat{a}_M)$, this leads to the following optimization problem:

$$\min_{\hat{\mathbf{A}}} F(\hat{\mathbf{A}}) \triangleq \alpha \hat{\Delta}(\hat{\mathbf{A}}) + (1 - \alpha) S(\hat{\mathbf{A}}) \quad (14a)$$

$$\text{s.t. } \text{tr}(\hat{\mathbf{A}}) = MT, \quad \hat{\mathbf{A}} \succeq \mathbf{0}, \quad (14b)$$

where $\alpha \in [0, 1]$ is the weighting factor that implicitly incorporates the necessary normalization to commensurate the disparate orders of magnitude of the two metrics, $\hat{\Delta}(\hat{\mathbf{A}})$ denotes the loss $\Delta(\mathbf{A})$ expressed in terms of $\hat{\mathbf{A}} = \mathbf{A}^2$, and $S(\hat{\mathbf{A}}) = \sum_{i=1}^M (\lambda_i^{-1} + \kappa \hat{a}_i)^{-1}$ denotes the sensing metric.

Proposition 3. *Problem (14) is a convex optimization problem with respect to $\hat{\mathbf{A}}$.*

Proof. (sketch) The objective is convex since $-\log \det(\hat{\mathbf{A}})$ is convex on the positive semidefinite cone and $S(\hat{\mathbf{A}})$ is a sum of convex functions in \hat{a}_i , while the constraint is affine. For a detailed proof, please refer to Appendix B. \square

The optimal power allocation $\hat{\mathbf{A}}^*$ is computed via a projected gradient algorithm (PGA). The gradient $\mathbf{G} = \nabla F(\hat{\mathbf{A}})$ is a diagonal matrix with entries:

$$[\mathbf{G}]_{ii} = -\frac{\alpha(1 - \frac{M}{T})}{\hat{a}_i} - \frac{(1 - \alpha)\kappa}{(\lambda_i^{-1} + \kappa \hat{a}_i)^2}, \quad \forall i = 1, \dots, M. \quad (15)$$

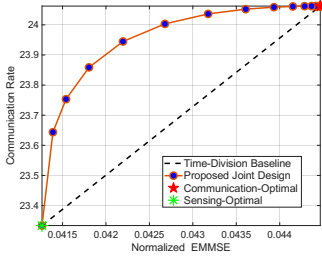


Fig. 1: The tradeoff between communication rate and normalized EMMSE.

In each iteration, the variable is updated via gradient descent followed by a projection \mathcal{P}_S onto the simplex constraint set $\{\hat{\mathbf{A}} \succeq \mathbf{0} \mid \text{tr}(\hat{\mathbf{A}}) = MT\}$. Upon convergence, the optimal solution is recovered as $\mathbf{A}^* = (\hat{\mathbf{A}}^*)^{1/2}$.

Simulation Results: We evaluate the proposed framework with $M = N_c = N_s = 8$, $T = 20$, $\text{SNR}_c = 20$ dB, and $\text{SNR}_s = 8$ dB, which accounts for the fact that radar sensing typically suffers from severe two-way path loss compared to the one-way communication link. According to Remark 1, when the sensing channel is isotropic, the S&C tradeoff vanishes. To explicitly demonstrate the non-trivial tradeoff behavior, we therefore consider a non-isotropic sensing channel model with $[\mathbf{R}_{\mathbf{H}_s}]_{ij} = N_s \rho^{|i-j|}$, where $\rho = 0.9$. We plot the normalized EMMSE, defined as $J_{\text{EMMSE}}/\text{tr}(\mathbf{R}_{\mathbf{H}_s})$, versus the communication rate $T^{-1}I_{\text{lb}} = C_{\text{pure}} - \Delta$. As illustrated in Fig. 1, there exists a clear Pareto frontier representing the tradeoff between S&C. Specifically, when $\alpha \rightarrow 1$, the system prioritizes the communication objective, driving the rate $T^{-1}I_{\text{lb}}$ to its maximum value C_{pure} , albeit at the cost of a significantly increased sensing metric. Conversely, as α decreases towards 0, the optimization shifts its focus toward sensing, resulting in a minimized EMMSE as the power allocation \mathbf{A} is optimized to align with the eigenvalues of $\mathbf{R}_{\mathbf{H}_s}$.

B. Asymptotic Analysis in the Low-SNR Regime

1) Power-Limited Communication and Flash Signaling:

Under the noncoherent block-fading model in Sec. II, the low-SNR capacity admits the first-order expansion [15], [16]

$$C(\text{SNR}_c) = N_c \log_2(e) \text{SNR}_c + o(\text{SNR}_c), \quad (16)$$

which coincides with the coherent benchmark to first order. Hence, to a first order, there is no capacity penalty for not knowing the channel at the receiver in the low-SNR regime, unlike in the high-SNR regime, where the noncoherent channel is degree of freedom limited.

Moreover, the first-order gain from multiple antennas comes from the increase in total received power due to multiple receive antennas (the linear factor N_c), whereas multiple transmit antennas provide no first-order improvement. The first-order term in (16) can be asymptotically achieved by *flash (temporally peaky) signaling*: allocating essentially all transmit energy in each coherence interval to a single symbol time and a single transmit spatial dimension (e.g., one transmit antenna/one beamforming direction), while the receiver adds up the received energies from the N_c antennas noncoherently.

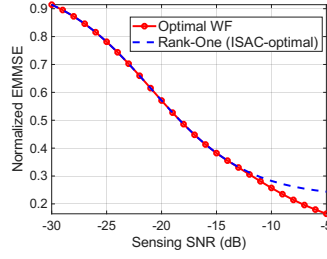


Fig. 2: Low-SNR sensing performance under different power allocation strategies.

2) *Low-SNR Sensing Behavior:* As $\text{SNR}_s \rightarrow 0$ (i.e., $\kappa \rightarrow 0$), the J_{EMMSE} in (5) can be approximated as

$$\begin{aligned} J_{\text{EMMSE}} &\stackrel{(a)}{=} \mathbb{E}_{\mathbf{X}} \left[\text{tr} \left(\mathbf{R}_{\mathbf{H}_s} - \kappa \mathbf{R}_{\mathbf{H}_s} \mathbf{X} \mathbf{X}^H \mathbf{R}_{\mathbf{H}_s} \right) \right] + o(\kappa) \\ &= \text{tr}(\mathbf{R}_{\mathbf{H}_s}) - \kappa \text{tr}(\mathbf{R}_{\mathbf{H}_s}^2 \boldsymbol{\Sigma}) + o(\kappa), \end{aligned} \quad (17)$$

where $\boldsymbol{\Sigma} = \mathbb{E}[\mathbf{X} \mathbf{X}^H]$, and (a) follows from the first-order matrix inverse expansion $(\mathbf{A}^{-1} + \kappa \mathbf{B})^{-1} = \mathbf{A} - \kappa \mathbf{A} \mathbf{B} \mathbf{A} + o(\kappa)$ for small κ [19]. Minimizing J_{EMMSE} is equivalent to solving

$$\max_{\boldsymbol{\Sigma} \succeq \mathbf{0}} \text{tr}(\mathbf{R}_{\mathbf{H}_s}^2 \boldsymbol{\Sigma}), \quad \text{s.t. } \text{tr}(\boldsymbol{\Sigma}) = MT. \quad (18)$$

Theorem 2. *In the low-SNR regime, a sensing-optimal $\boldsymbol{\Sigma}^*$ is rank-one and given by $\boldsymbol{\Sigma}^* = MT \mathbf{u}_{\text{max}} \mathbf{u}_{\text{max}}^H$, where \mathbf{u}_{max} is the dominant eigenvector of $\mathbf{R}_{\mathbf{H}_s}$.*

Proof. By von Neumann's trace inequality [19], $\text{tr}(\mathbf{R}_{\mathbf{H}_s}^2 \boldsymbol{\Sigma}) \leq \sum_{i=1}^M \lambda_i(\mathbf{R}_{\mathbf{H}_s}^2) \lambda_i(\boldsymbol{\Sigma}) \leq MT \cdot \lambda_{\text{max}}^2(\mathbf{R}_{\mathbf{H}_s})$, where $\lambda_i(\cdot)$ denotes eigenvalues in nonincreasing order. The upper bound is achieved by the rank-one $\boldsymbol{\Sigma}^* = MT \mathbf{u}_{\text{max}} \mathbf{u}_{\text{max}}^H$. \square

Corollary 1 (First-Order Optimal ISAC Signal Structure). *A first-order optimal ISAC waveform can be chosen to be rank-one in space and flash in time, e.g.,*

$$\mathbf{X}_{\text{opt}} = \sqrt{MT} \mathbf{u}_{\text{max}} \xi \mathbf{e}_1^T, \quad (19)$$

where $\mathbf{e}_1 \in \mathbb{C}^T$ is the first basis vector and $\xi \in \mathbb{C}$ is a random scalar satisfying $\mathbb{E}[|\xi|^2] = 1$ with a peaky/flash distribution (zero most of the time and very large with very small probability).

Remark 2 (Low-SNR Tradeoff Vanishing). *Corollary 1 satisfies $\mathbb{E}[\mathbf{X}_{\text{opt}} \mathbf{X}_{\text{opt}}^H] = MT \mathbf{u}_{\text{max}} \mathbf{u}_{\text{max}}^H$ and is therefore sensing-optimal to first order by (17). Meanwhile, it follows that allocating all transmit energy in each coherence interval to a single symbol and a single transmit spatial dimension is sufficient to asymptotically achieve the first-order term in (16). Since the channel is isotropic, choosing the direction as \mathbf{u}_{max} incurs no first-order communication loss. Hence, the S&C tradeoff vanishes asymptotically to first order at low SNR.*

Simulation Results: We evaluate the normalized EMMSE in the low-SNR regime, to illustrate the accuracy of the asymptotic analysis. The system parameters are set to $M = N_s = 8$ and $T = 20$, with the same $\mathbf{R}_{\mathbf{H}_s}$ as in Fig. 1. Specifically, Fig. 2 compares two spatial power allocation strategies: (i) the sensing-optimal water-filling solution in Proposition 1, and (ii) the rank-one signaling strategy predicted by Corollary 1. As SNR_s decreases, the performance gap between the water-filling solution and the rank-one strategy gradually vanishes. This convergence empirically confirms that the rank-one spatial structure becomes asymptotically optimal in the low-SNR regime. The communication performance is not explicitly plotted because, to first order as $\text{SNR}_c \rightarrow 0$, the achievable rate is governed by the total transmit energy. Under the same block-energy constraint and the same temporally peaky/flash signaling pattern, different spatial covariances do not affect the first-order term in the low-SNR expansion.

V. CONCLUSION AND DISCUSSION

This paper provided a new perspective on the fundamental limits of noncoherent ISAC systems. Contrary to the conventional intuition that communication and sensing are inherently conflicting, our analysis revealed that their structural alignment is highly SNR-dependent. Specifically, the identified vanishing tradeoff phenomenon—occurring not only in the low-SNR regime but also under specific high-SNR configurations—suggests that joint signaling can achieve near-optimal performance for both functionalities simultaneously. This convergence implies that the perceived mismatch between the USTM signaling and sensing-optimal power allocation is a flexible constraint rather than a fundamental barrier.

ACKNOWLEDGEMENT

The work of H. Yang and K. Wan was funded by NSFC-12141107 and Wuhan “Chen Guang” Program under Grant 2024040801020211, and the work of G. Caire was supported by the Gottfried Wilhelm Leibniz-Preis 2021 of the German Science Foundation (DFG).

APPENDIX A

PROOF OF PROPOSITION 1

Recalling the definition in (5), let

$$f(\mathbf{R}_\mathbf{x}) = \text{tr}((\mathbf{R}_{\mathbf{H}_s}^{-1} + \kappa T \mathbf{R}_\mathbf{x})^{-1}).$$

The mapping $\mathbf{S} \mapsto (\mathbf{R}_{\mathbf{H}_s}^{-1} + \kappa T \mathbf{S})^{-1}$ is matrix convex on the positive semidefinite cone, and the trace operator is linear; hence $f(\cdot)$ is convex in $\mathbf{R}_\mathbf{x} \succeq \mathbf{0}$. By Jensen’s inequality,

$$\mathbb{E}[f(\mathbf{R}_\mathbf{x})] \geq f(\mathbb{E}[\mathbf{R}_\mathbf{x}]) \triangleq f(\tilde{\mathbf{R}}_\mathbf{x}),$$

with equality if $\mathbf{R}_\mathbf{x}$ is deterministic, i.e., $\mathbf{R}_\mathbf{x} = \tilde{\mathbf{R}}_\mathbf{x}$ almost surely. This proves Item 1).

For a deterministic $\mathbf{R}_\mathbf{x}$, the objective $f(\mathbf{R}_\mathbf{x})$ is minimized when its eigenvectors align with those of $\mathbf{R}_{\mathbf{H}_s}^{-1}$, equivalently with those of $\mathbf{R}_{\mathbf{H}_s}$, by the standard trace/eigenvalue alignment argument. This yields Item 2). Substituting the eigendecompositions into $f(\cdot)$ reduces the problem to the scalar convex optimization

$$\min_{\{d_i \geq 0\}} \sum_{i=1}^M (\lambda_i^{-1} + \kappa T d_i^2)^{-1}, \quad \text{s.t.} \quad \sum_{i=1}^M d_i^2 = M.$$

The KKT conditions give

$$(d_i^*)^2 = \frac{1}{\kappa T} \left(\nu - \frac{1}{\lambda_i} \right)^+, \quad i = 1, \dots, M,$$

where ν is chosen such that $\sum_{i=1}^M (d_i^*)^2 = M$. This proves Item 3). Item 4) follows directly when $\mathbf{R}_{\mathbf{H}_s} \propto \mathbf{I}_M$, in which case the symmetry of the scalar problem gives $d_i^* = 1$ for all $i = 1, \dots, M$.

APPENDIX B

PROOF OF PROPOSITION 3

Using the definition of the sensing-induced rate loss, the term $\hat{\Delta}(\hat{\mathbf{A}})$ can be written, up to constants independent of $\hat{\mathbf{A}}$, as

$$\hat{\Delta}(\hat{\mathbf{A}}) = - \left(1 - \frac{M}{T} \right) \log \det(\hat{\mathbf{A}}) + \text{const.}$$

Since $-\log \det(\hat{\mathbf{A}})$ is convex on the positive definite cone, $\hat{\Delta}(\hat{\mathbf{A}})$ is convex on its domain. The sensing objective is separable:

$$S(\hat{\mathbf{A}}) = \sum_{i=1}^M s_i(\hat{a}_i), \quad s_i(\hat{a}_i) = (\lambda_i^{-1} + \kappa \hat{a}_i)^{-1}.$$

For $\hat{a}_i \geq 0$, its second derivative is

$$s_i''(\hat{a}_i) = \frac{2\kappa^2}{(\lambda_i^{-1} + \kappa \hat{a}_i)^3} \geq 0,$$

so each $s_i(\cdot)$ is convex and therefore $S(\hat{\mathbf{A}})$ is convex. For any $\alpha \in [0, 1]$, $F(\hat{\mathbf{A}}) = \alpha \hat{\Delta}(\hat{\mathbf{A}}) + (1 - \alpha)S(\hat{\mathbf{A}})$ is a nonnegative weighted sum of convex functions. Finally, the feasible set

$$\{\hat{\mathbf{A}} \succeq \mathbf{0} \mid \text{tr}(\hat{\mathbf{A}}) = MT\}$$

is convex because it is the intersection of the positive semidefinite cone and an affine hyperplane. Thus, Problem (14) is convex with respect to $\hat{\mathbf{A}}$.

REFERENCES

- [1] Y. Xiong, F. Liu, Y. Cui, W. Yuan, T. X. Han, and G. Caire, “On the fundamental tradeoff of integrated sensing and communications under Gaussian channels,” *IEEE Trans. Inf. Theory*, vol. 69, no. 9, pp. 5723–5751, Sep. 2023.
- [2] M. Ahmadipour, M. Kobayashi, M. Wigger, and G. Caire, “An information-theoretic approach to joint sensing and communication,” *IEEE Trans. Inf. Theory*, vol. 70, no. 2, pp. 1124–1146, Feb. 2024.
- [3] G. Yilmaz, F. Lampel, H. Joudeh, and G. Caire, “Joint communication and parameter estimation in MIMO channels,” *IEEE J. Sel. Areas Inf. Theory*, vol. 7, pp. 91–105, Mar. 2026.
- [4] Y. Guo, Y. Gu, M. Wang, and B. Xia, “Fundamental limits for ISAC: CRB-rate bound and bound-achieving input distribution,” *IEEE Trans. Wireless Commun.*, pp. 1–1, 2025.
- [5] Z. Wang and X. Wang, “Fundamental MMSE-rate performance limits of integrated sensing and communication systems,” arXiv preprint, arXiv:2501.01053, 2025.
- [6] X. Shen, Z. Lu, N. Zhao, H. Zhao, and Y. Shen, “Fundamental tradeoff of bistatic ISAC under Gaussian fading channels at finite blocklength,” *IEEE Trans. Inf. Theory*, pp. 1–1, 2025.
- [7] Z. Yu, X. Hu, C. Liu, and M. Peng, “Rethinking the fundamental performance limits of integrated sensing and communication systems,” *IEEE Trans. Wireless Commun.*, vol. 24, no. 11, pp. 9311–9322, 2025.
- [8] M. Kobayashi, H. Hamad, G. Kramer, and G. Caire, “Joint state sensing and communication over memoryless multiple access channels,” in *Proc. IEEE Int. Symp. Inf. Theory (ISIT)*, Jul. 2019, pp. 270–274.
- [9] F. Liu, Y. Xiong, K. Wan, T. X. Han, and G. Caire, “Deterministic-random tradeoff of integrated sensing and communications in Gaussian channels: A rate-distortion perspective,” in *Proc. IEEE Int. Symp. Inf. Theory (ISIT)*, Jun. 2023, pp. 2326–2331.
- [10] Z. Du, F. Liu, Y. Xiong, T. X. Han, Y. C. Eldar, and S. Jin, “Reshaping the ISAC tradeoff under OFDM signaling: A probabilistic constellation shaping approach,” *IEEE Trans. Signal Process.*, vol. 72, pp. 4782–4797, 2024.
- [11] W. Zhang, S. Vedantam, and U. Mitra, “Joint transmission and state estimation: A constrained channel coding approach,” *IEEE Trans. Inf. Theory*, vol. 57, no. 10, pp. 7084–7095, Oct. 2011.
- [12] C. Choudhuri, Y.-H. Kim, and U. Mitra, “Causal state communication,” *IEEE Trans. Inf. Theory*, vol. 59, no. 6, pp. 3709–3719, Jun. 2013.
- [13] M.-C. Chang, S.-Y. Wang, T. Erdoğ̃an, and M. R. Bloch, “Rate and detection-error exponent tradeoff for joint communication and sensing of fixed channel states,” *IEEE J. Sel. Areas Inf. Theory*, vol. 4, pp. 245–259, May 2023.
- [14] B. M. Hochwald and T. L. Marzetta, “Unitary space-time modulation for multiple-antenna communications in Rayleigh flat fading,” *IEEE Trans. Inf. Theory*, vol. 46, no. 2, pp. 543–564, Mar. 2000.
- [15] L. Zheng and D. N. C. Tse, “Communication on the Grassmann manifold: a geometric approach to the noncoherent multiple-antenna channel,” *IEEE Trans. Inf. Theory*, vol. 48, no. 2, pp. 359–383, Feb. 2002.

- [16] S. Verdú, "Spectral efficiency in the wideband regime," *IEEE Trans. Inf. Theory*, vol. 48, no. 6, pp. 1319–1343, Jun. 2002.
- [17] S. Lu, F. Liu, F. Dong, Y. Xiong, J. Xu, Y.-F. Liu, and S. Jin, "Random ISAC signals deserve dedicated precoding," *IEEE Trans. Signal Process.*, vol. 72, pp. 3453–3469, 2024.
- [18] T. Marzetta and B. Hochwald, "Capacity of a mobile multiple-antenna communication link in rayleigh flat fading," *IEEE Trans. Inf. Theory*, vol. 45, no. 1, pp. 139–157, Jan. 1999.
- [19] R. A. Horn and C. R. Johnson, *Matrix analysis*. Cambridge university press, 2012.